10th International Conference on Composite Science and Technology
ICCST/10
A.L. Araújo, J.R. Correia, C.M. Mota Soares, et al. (Editors)

INTERFACIAL SLIDING IN COMPOSITE INTERFACES AT ELEVATED HOMOLOGOUS TEMPERATURES: OBSERVATIONS IN 3D ELECTRONIC DEVICES

I. Dutta[*], L. Meinshausen[*], M. Liu[*], T. K. Lee[†]

[*] School of Mechanical and Materials Engineering, Washington State University, Pullman, WA
idutta@wsu.edu; lutz.meinshausen@wsu.edu; ming.liu2@wsu.edu

[†] Cicso Systems Inc., San Jose, CA, USA
taeklee@cisco.com

Key words: Interface, Diffusion, Sliding, Electromigration, Thermal Cycling, Microelectronics, Through-Silicon Vias.

Summary: *Diffusionally accommodated interfacial sliding between a metal and an inorganic non-metal has been analytically modeled and experimentally studied previously. This phenomenon occurs when the metallic component of the composite (or laminate) is heated to a high enough homologous temperature (T/T_M) where diffusional processes such as creep become important. Chemical potential differences created along the length of the interface drive diffusional flux, and makes one component of the composite (e.g., the fiber) slide relative to the other (e.g., the matrix). This effect can cause fiber-ends to protrude or intrude relative to the matrix, or for thin film lines to migrate relative to a substrate. The effect becomes increasingly important with decreasing scale, and can be of substantial impact in next-generation electronic devices, where cylindrical Cu (copper) through-silicon-vias (TSVs) are embedded in a Si (silicon) device. This paper first reviews the constitutive model for interfacial sliding under applied stress and voltage gradients, and then reports experimental results on these effects in TSV-Si composites.*

1 INTRODUCTION

The elevated temperature mechanical properties of interfaces between dissimilar materials are critical to the performance of a wide range of engineering systems, such as microelectronic devices, film-substrate systems, and composites. In many such applications, large shear stresses exist at the interface, and at least one of the materials adjacent to the interface is subjected to a high homologous temperature (T/T_m). This enables *diffusionally accommodated sliding* processes (interfacial creep) to operate at the interface [e.g., 1-16], impacting the deformation behavior, dimensional stability, and reliability of the component.

Recently, substantial advances have been made in experimentally measuring interfacial sliding in various model systems [3,17-20], and the key phenomenological aspects of a previously developed kinetics law [3] have been experimentally validated [17,19]. In addition, the impact of interfacial sliding during thermo-mechanical deformation has been studied experimentally and analytically in metal-matrix composites [4,5], thin film/substrate

systems [21-23], and metal/dielectric interconnect structures in microelectronic devices [24-29]. This paper discusses the impact of interfacial sliding in the context of the emerging field of 3-dimensional (3D) electronic packaging.

In 3D packages, numerous Cu-filled through-silicon vias (TSVs), which are typically 10-100μm in diameter, run through the thickness of a Si electronic device (chip), providing electrical interconnection between multiple chips, which are stacked on top of each other. In addition to reducing the footprint of the overall electronic component, this architecture results in much shorter communication bus-lengths, which results in faster performance and much lower energy consumption. The interfaces between Cu and Si, however, are subject to diffusional sliding, which can lead to intrusion/protrusion of the Cu relative to Si during thermal cycling, or when an electric current is passed through the TSVs [30,31]. Thermal activation for interfacial diffusion is provided by Joule heating, whereas the driving force for diffusion is provided by stress-gradients due to the thermal expansion mismatch between Cu and Si, or by the voltage-gradient associated with the current passing through the TSV. Experiments conducted on 100μm diameter TSVs embedded in a Si chip with a <1μm thick SiO_2 barrier layer at the interface showed that: (a) during thermal cycling (TC), the ends of the TSV may either protrude from or intrude into the Si by a small distance (nanometer to micrometer range) due to interfacial sliding close to the ends as a result interfacial shear stresses developed via shear-lag; (b) interfacial sliding also occured due to electromigration driven diffusional flux along the interface, resulting in the overall migration of TSVs in the direction of electron flow.

In this paper, we first present the phenomenon of interfacial sliding, as driven by a combination of applied shear stress and electric field. Then, we present experimental results and FEM simulation of interfacial sliding in a new generation Si-chips containing an array of 10μm diameter Cu TSVs, where the interfaces have been engineered with a proprietary dielectric buffer-layer (to reduce interfacial stresses) and an adhesion-enhancing diffusion-barrier layer.

2 CONSTITUTIVE MODEL FOR INTERFACIAL SLIDING

When a far-field shear stress is applied to a hetero-interface, local normal stress gradients are set up along the interface, which causes mass flow to occur via diffusional transport along the interface. Typically, the activation energy for this transport is very low (~1/2 that for volume diffusion in the lower-melting metallic component adjacent to the interface) [3,17,19,32], suggesting that (a) the interface serves as a short-circuit path for diffusion, and (b) the interface is a prolific source of vacancies, thus preempting the requirement to form vacancies prior to their movement. In some systems (e.g., Al-Si), the presence of a very thin amorphous interfacial layer (~a few nm) produces an open structure, through self-diffusion of atoms can proceed rapidly, possibly reducing the need for vacancies [19]. When a large electric current density is superimposed on the metallic component (which may be an interconnect line or a TSV), the electric field causes an EM-induced mass flow along the interface (particularly when the grain size of the metallic component is large compared to the line-width or TSV-diameter, such that grain boundary diffusion is suppressed), leading to net mass-transfer from the cathode (-) to the anode (+), in the direction of the electron-wind force (F_{wd}). When the direction of electron flow is along the applied shear stress on the metal side of the interface, the two driving forces (due to τ_i and the electric field E, which equals $j\rho$,

where ρ is the resistivity of the metal) act in concert to enhance the rate of sliding. Conversely, the sliding rate decreases if electron-flow is opposite to the shear stress direction on the metal side, which causes the stress and electromigration-induced fluxes to counteract each other.

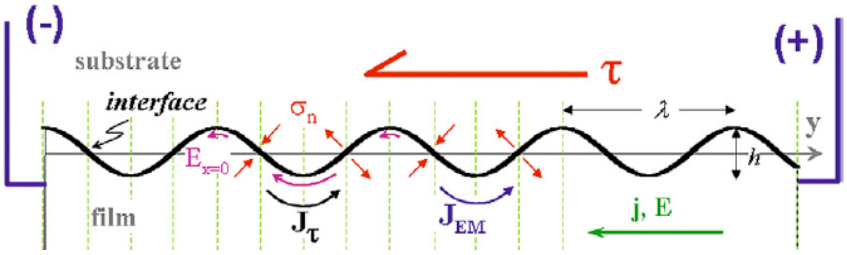

Figure 1: Schmatic of an undulating (periodic) interface between a metallic component (film) and a non-metallic component (substrate), with an applied shear stress pushing the substrate to the left and the film to the right. τ_i is positive when acting in the +y direction in the metal film. A current flows in the metal film along the electric field E, which is from right to left. This drives an EM flux (J_{EM}), which is driven by electron flow, along the interface from left to right. The interfacial flux due to τ_i ($J\tau$) is also from left to right. In this instance, $J\tau$ and J_{EM} augment each other.

Representing the interface as an undulating surface (e.g., with Si on one side, and Cu on the other, **Figure 1**), the interfacial sliding rate, $\dot{U}$, due to both τ_i and E is given by [32]:

$$\dot{U} = \frac{4\Omega\lambda\tau_i}{\pi kTh^2}\left(D_f^{eff} + \frac{2\pi\delta_i D_i}{\lambda}\right) + \frac{2\lambda Z^* eE}{\pi kTh}\left(D_f^{eff} + \frac{2\pi\delta_i D_i}{\lambda}\right) \quad (1)$$

where Ω is the atomic volume, λ and h are the wavelength and the distance between the trough and the crest of the periodic, undulating interface, respectively, k and T are the Boltzaman constant and temperature, respectively, D_f^{eff} and D_i are the effective diffusion coefficient for diffusion through film and interfacial diffusion coefficients, respectively, δ_i is the width of the interfacial region, and Z* and e are the effective charge number of the diffusing ion and the charge of an electron, respectively. Note that Z* is a negative number (a typical value is -27 for Al). When $D_i >> D_f^{eff}$ (e.g., when grain boundary flux is negigible because of the large grain size of the metal, and temperature is low enough that volume diffusion flux is not large), Equation (1) is simplified as follows [32]:

$$\dot{U} = \frac{8\Omega\delta_i D_i}{kTh^2}\tau_i + \frac{4\delta_i D_i}{kTh}Z^* eE \quad (2)$$

Thus, $\dot{U}$ depends linearly on both τ_i and E, the relative signs of which determining whether they augment or mitigate each other's contributions. Since Z* is negative, the second term (due to EM) acts against the first term (due to stress-driven creep) when both driving forces (τ_i and E) are positive, and thus reduce the interfacial sliding rate. Conversely, if τ_i and E have opposite signs, the two terms in eqn. 2 augment each other and increase interfacial sliding kinetics.

Eqn. 2 also shows that the EM component has a smaller dependence on interfacial roughness (h) than the stress component. Therefore, for smoother interfaces, the stress component usually dominates, whereas for less smooth interfaces, the EM component is expected to play a stronger role. The above theoretically derived results were experimentally validated [32] based on sandwich samples of Si-Pb-Si, where the Si-Pb interfaces were

observed to undergo sliding in a predictable manner due to either stress, or EM, or due to stress and EM combined. Additional details of the model and experiments are given in [32].

In the following, we present experimental and modeling results to assess the impact of stress and electromigration driven interfacial sliding in the Cu-TSV / Si system.

3 EXPERIMENTAL AND MODELING PROCEDURES

3.1 Experiments

100μm thick Si chips with large arrays of 10μm diameter Cu-filled TSV were used for the experiments. Both surfaces of the chips were metallographically polished to remove the redistribution layers (RDL), such that the ends of the TSVs were nominally flush with the Si at both surfaces. Because of differences in the hardness (and hence polishing rate) between Cu an Si, the TSVs protruded slighly from the Si even before testing. The height difference between the TSV-end and surrounding Si ($\Delta l = L_{TSV} - L_{Si}$) was measured using scanning white light interferometer (SWLI) and the Cu/Si interface was observed in a scanning electron microscope (SEM), before and after experiments (thermail cycling or electromigration).

Micrographs of the sample is shown in **Figure 2**.

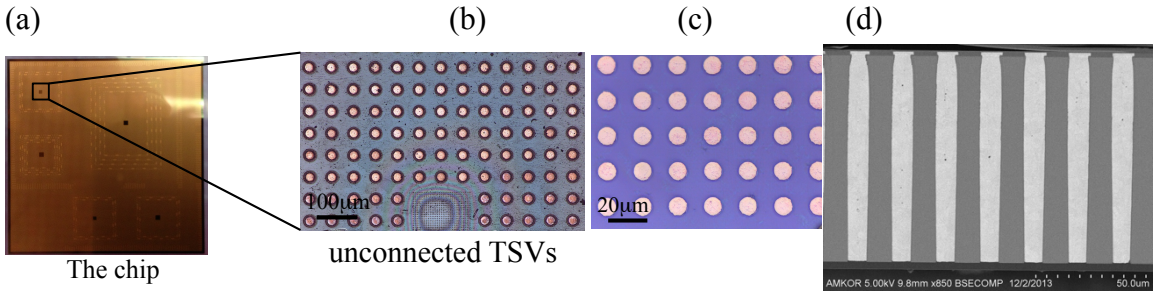

Figure 2: (a) View of the top-surface of a test chip, showing an array of TSVs (b,c), and a cross-sectional view of the TSVs in the chip (d). The system is a composite containing Cu fibers in a Si matrix.

The samples were thermally cycled between -25°C and 150°C with heating and cooling rates of 0.1°C/s and a dwell-time of 10 minutes at each temperature extremity. This slow thermal cycling rate was devised to allow sufficient time for creep (i.e., diffusional relaxation mechanisms) to operate during cycling, so as to elucidate the effect of interfacial sliding.

In addition to the thermal cycling tests, the TSVs were also subjected to electromigration tests, wherein Cu thin films were deposited on the top and bottom surfaces of the chip, and separate electrical leads were attached to the top and bottom films. An electric field was applied to these leads such that a current flowed through each TSV in parallel. The applied current density to each TSV was s $5 \times 10^5 A/cm^2$. The entire test was conducted in high vacuum, at 120°C and 170°C and times of 12 to 118 hours, and EM-induced sliding was investigated by characterizing the relative displacement between the TSV-end and Si.

3.2 Finite Element Modeling

A non-linear, 2-dimensional axisymmetric finite element model (FEM) of a single TSV in a cylindrical Si matrix was constructed in the y-z plane, with z being the fiber axis. Appropriate boundary conditions were applied, such that the model acts as a unit cell in a

large body comprising many such cells.

Table 1: Properties used in FEM

Property	**Copper**	**Si**
Melting temperature (K)	1356	N/A
Thermal expansion coefficient (1/K)	17 x 10^{-6}	3 x 10^{-6}
Young's modulus (GPa)	$E = 115\left[1-\left(T-300\right)/T_{\mathrm{m}}\right]$	130
Poisson's ratio	0.3	0.28
Yield strength (MPa)	$\sigma_{\mathrm{y}} = 250\sqrt{\exp\left[-10\left(T-296\right)/1000\right]}$	
Linear work hardening modulus (MPa)	$E_{\mathrm{t}} = 1000\left(1-\left(T-300\right)/T_{\mathrm{m}}\right)$	
Power-law creep of Cu (shear strain rate):	$\dot{\gamma}_{PL} = A_2 D_{\mathrm{eff}} \frac{\mu b}{kT}\left(\tau/\mu\right)^n$ where $D_{\mathrm{eff}} = D_{\mathrm{v}}\left[1+\frac{10a_{\mathrm{c}}}{b^2}\left(\tau/\mu\right)^2\frac{D_{\mathrm{c}}}{D_{\mathrm{v}}}\right]$, $D_v = D_{0v}\exp\left(-\frac{Q_v}{RT}\right)$, $\delta D_{\mathrm{gb}} = \delta D_{0\mathrm{gb}}\exp\left(-\frac{Q_{\mathrm{gb}}}{RT}\right)$, $a_c D_c = a_c D_{0c}\exp\left(-\frac{Q_c}{RT}\right)$	
Coble creep of Cu (shear strain rate):	$\dot{\gamma}_C = 42\frac{\tau_i \Omega}{kT}\frac{\pi\delta_{gb}D_{gb}}{d^3}$	
Relationship between normal & shear stresses and strain rates	$\tau = \frac{\bar{\sigma}}{\sqrt{3}}, \dot{\gamma} = \sqrt{3}\dot{\varepsilon}$	
Pre-exponential and activation energy for core diffusion: $\delta_C D_{C0}$ (m^3/s), Q_c (kJ/mole)	1x10^{-24}, 117	
Pre-exp. and act. energy for grain bdy. diffusion, $\delta_{gb}D_{gb0}$ (m^3/s), Qc (kJ/mole)	5 x 10^{-15}, 104	
Cu grain size	1 μm	
Cu Burgers vector	2.5x10^{-10}m	
Cu atomic volume, Ω (m^3)	1.18 x 10^{-29}	
Electrical resistivity of copper (nΩm)	ρ= 16.8 (1+3.9 x 10^{-3}(T-273))	
Cu-TSV Diameter (μm)	10	
Cu-TSV Initial length (μm)	100	
Interfacial Properties (all mechanical properties same as Cu)		
Creep of Interface (shear strain rate):	$\dot{\gamma}_{\mathrm{i}} = A_{\mathrm{i}}\tau_{\mathrm{i}}$ where $A_{\mathrm{i}} = \frac{8\delta_{\mathrm{i}}D_{0\mathrm{i}}\Omega}{kTh^3}\exp\left(-\frac{Q_{\mathrm{i}}}{RT}\right)$	
Pre-exp and activation energy for interface diffusion: $\delta_i D_{i0}$ (m^3/s), Qi (kJ/mol)	10^{-4} $\delta_{gb}D_{gb0}$, 55kJ/mole	
Activation energy for interfacial diffusion, Q (kJ/mole)	55	
Interfacial roughness: h (m)	0.1μm	
Interfacial roughness to period ratio: h/λ	0.1	

The model comprised one quadrant of the cell, with the Cu-TSV being 5μm in radius and 50μm in helf-length (since the chip is 100μm in thickness). A separate 0.1μm thick interfacial layer, with identical properties as Cu, but following the creep behavior in eqn. (1),

was present between the Cu-TSV and Si. The model had about 80,000 elements. The boundary conditions imposed were: (i) z displacement = 0 along y=0, (ii) y displacement = 0 along y=0; (iii) the walls of the interface layer with Cu and Si, as well as the radial boundary of the cell remained straight. The model is depicted in **Figure 3**.

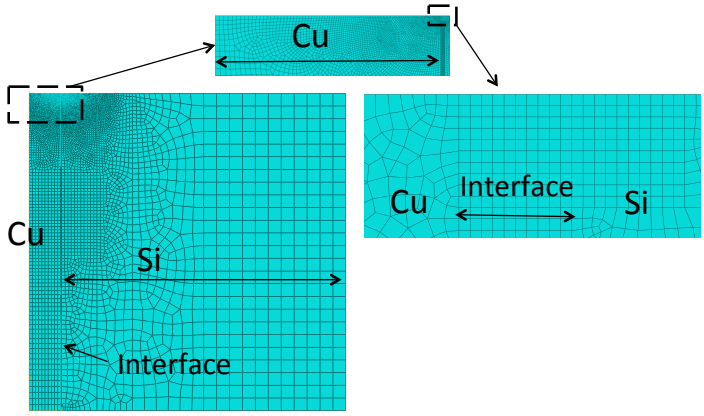

Figure 3: Finite element model of the Cu-Si unit cell, with a separate third layer in between representing the interface. Boxes denote the regions which are shown inthe enlarged views .

The Cu and the interfacial zone were assumed to be elastic-plastic-creeping, and Si was elastic. Cu was assumed to creep by power-law creep via both lattice and dislocation core diffusion, as well as by grain boundary diffusion-controlled Coble creep. The interface crept by the first term of equation 1 (since E=0), with all other properties identical to those of Cu. Table 1 summarizes the properties used in the FEM.

Simulations were conducted both without and with initial residual stresses at the start of cycling. To simulate the effect of residual stress, the stress-free model at 20^{o}C is heated to 400^{o}C (corresponding to the temperature of RDL deposition), held for 10 minutes, cooled to 20^{o}C at 10^{o}C/minute, held at 20oC for 24 hours, and then cycled from -25^{o}C to 150^{o}C. For the case without initial residual stress, the sample was cooled from 20^{o}C to -25^{o}C, and then cycled from -25^{o}C to 150^{o}C with ramp rates of 0.1^{o}C/min and dwell time of 10 mins at the temperature extremities. Simulations were also conducted without a viscous interface layer, where the interface layer was simply assumed to have identical creep properties as Cu. For the sake of brevity, only the results based on the model with interfacial sliding and without initial residual stresses are presented in this paper, but the inferences are drawn based on all the results.

4 RESULTS AND DISCUSSION

4.1 Interfacial Sliding during Thermal Cycling: Experiments and Modeling

Figure 4 shows the relative displacement between the top of the Cu TSV and Si as a function of the number of thermal cycles to which the sample is subjected. It is observed that at the beginning of cycling, the Cu TSV protrudes out of the Si surface by about 25 nm. This is an artifact of the polishing method that was used to prepare the samples. During the initial few cycles, the TSV shrinks relative to the Si, and after 5 cycles, intrudes into the Si by about

5 nm. But during continued cycling, the TSV expands and starts protruding from the Si. Up to about 20 cycles, the expansion is quite rapid, following which it slows down. It is noted that the relative displacement was measured along three lines drawn at 120° from each other, and the data (and associated scatter) reported represent the displacements along these lines for 4 TSVs, relative to the surrounding Si. It should be further noted that this effect is symmetric at both ends of the TSV.

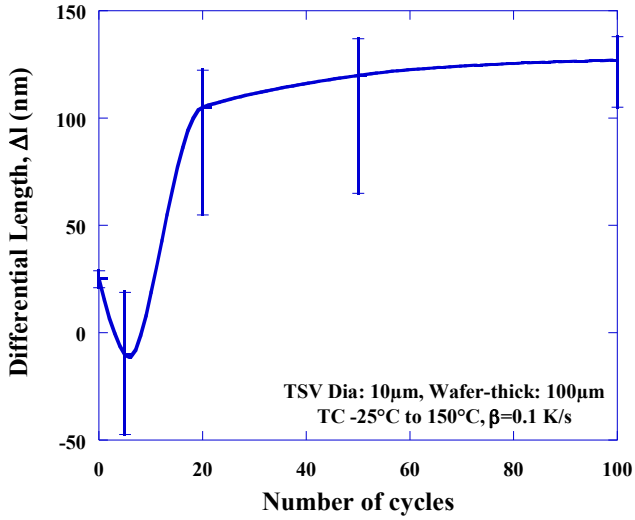

Figure 4: Mean displacement of the top of the Cu-TSV relative to Si. The TSVs initially intrude into Si for the first few cycles, and then start protruding. The protrusion stabilizes after ~60 cycles.

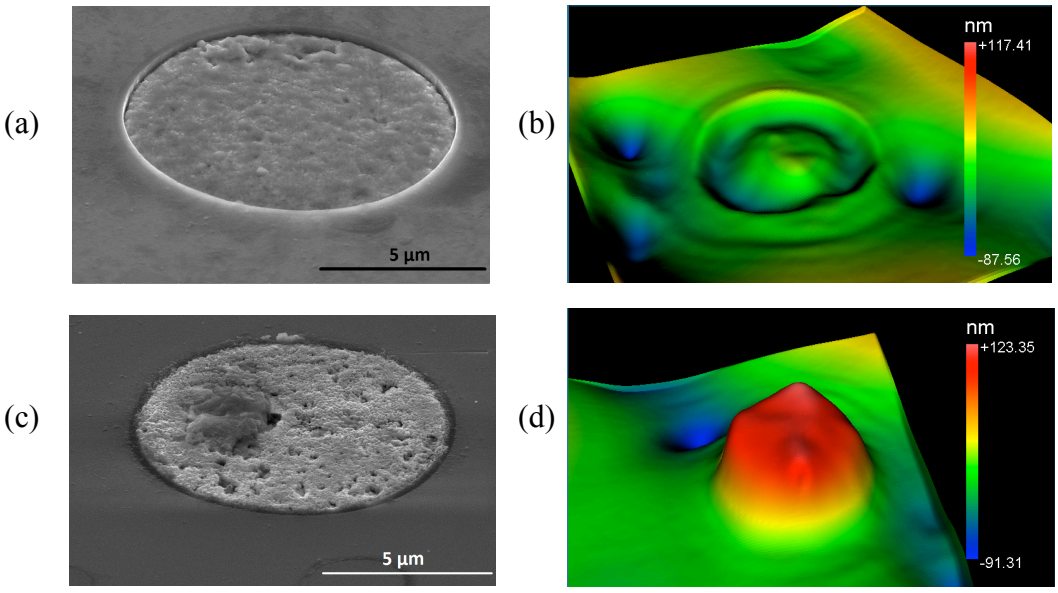

Figure 5: Scanning electron micrographs (a, c) and optical profiles (b,d) of a TSV in Si after 5 cycles (a,b) and 100 cycles (b,d). The TSV intrudes into Si after 5 cycles, and protrudes after 100 cycles.

Figure 5a and 5b show an SEM image and a SWLI profile of the top of a Cu TSV after 5 cycles, respectively. Clearly, the TSV intrudes into Si after 5 cycles. This may be due to

annealing-related grain boundary defect elimination, and/or relief of fabrication-related residual stresses. Electroplated Cu films on Si are known to contain defects such as contaminants at grain boundaries, microvoids at boundaries and triple grain junctions, and also have signficant stress immediately after deposition. But these films undergo self-annealing, which can cause recrystallization and grain growth, changes in crystallographic texture, stress-relief, and a decrease in resistivity [33], and it is possible that the shrinkage is related to this. Importantly, however, as evident from the SEM picture, the elevation difference between TSV and the surrounding Si is sharp (and greatest) at the interface, clearly indicating that the relative shrinkage of Cu is accommodated at the interface by sliding.

Figures 5c and 5d show an SEM picture and a surface profile of a TSV after 100 cycles. As observed in Figure 4, here the TSV protrudes quite signficantly from the Si surface (by >100nm). Clearly, the step is large and sharp at the interface, again suggesting sliding of the interface. It is important to differentiate between this inference (i.e., that interfacial has occured), versus what would have happened if the Cu had simply undergone expansion without interfacial sliding. If the latter were true, and the interface was perfectly bonded and non-sliding, there would be no step at the interface, and the height difference would increase as one moved towards the center of the TSV. In other words, the greatest difference in height would be found between the TSV-axis and the Si, quite unlike what is clearly observed in **Figure 5b**. It is therefore evident that diffusionally accommodated interfacial sliding is a critical event in these fiber-reinforced composites. It is further noted that although there are grain boundaries inside the TSV, the interfaces still provide a faster path for diffusion, even in these interfacially-engineered next-generation devices.

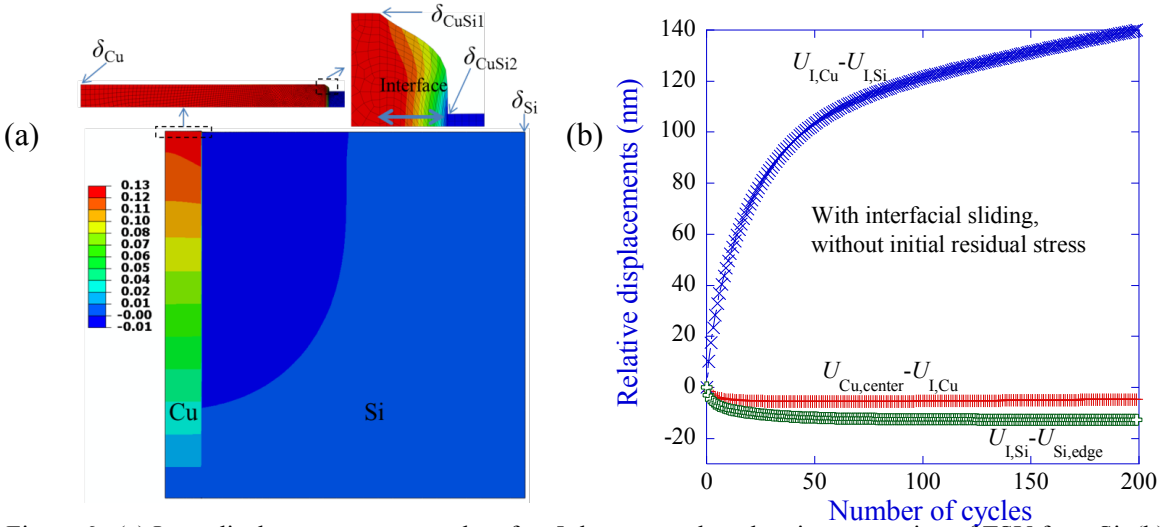

Figure 6: (a) Iso z-displacement contour plot after 5 thermal cycles, showing protrusion of TSV from Si; (b) Relative displacement of the Cu and Si immediately across the 'interface' and between the center of the Cu TSV and Si. Both figures show that with nearly all differential deformation occurs at the interface due to interfacial creep or interfacial sliding.

In the following, we present a model-based rationalizaton of the above experimental results. **Figure 6a** shows a contour plot of constant z-displacement in the FE unit cell for the model with interfacial sliding, but without an initial residual stress. The Cu-TSV is observed to protrude out of the Si surface, as clearly observed in the blow-up of the interface region

(top right of **Fig. 6a**). Importantly, the displacement is observed to be entirely accommodated at the interface, with the top of the Cu-TSV remaining nominally flat, as seen experimentally. This is more clearly observed in **Figure 6b**, which shows that the relative displacement between the tops of the Cu and Si across the interfacial zone increases progressively with continued cycling, whereas the relative displacement between the center and circumference of the Cu-TSV remains constant near zero with cycling. Clearly, the protrusion occurs due to sliding at the interface, as opposed to due to only deformation of the Cu with a perfect, non-sliding interface. We also note that the surface profile of the Cu-TSV in the absence of a creeping interfacial zone (i.e., sliding interface) is substantially curved, in contrast to **Figure 6a**.

4.2 Interfacial Sliding during Electromigration: Experiments

Above, we showed that during thermal cycling, both ends of the TSV either intrude into, or protrude out from the Si surface symmetrically due to shear-lag induced shear stresses at the interface. In the following, we show that in contrast to the symmetric incompatibility that is seen after thermal cycling, electromigration results in intrusion at one end, and protrusion from the other end.

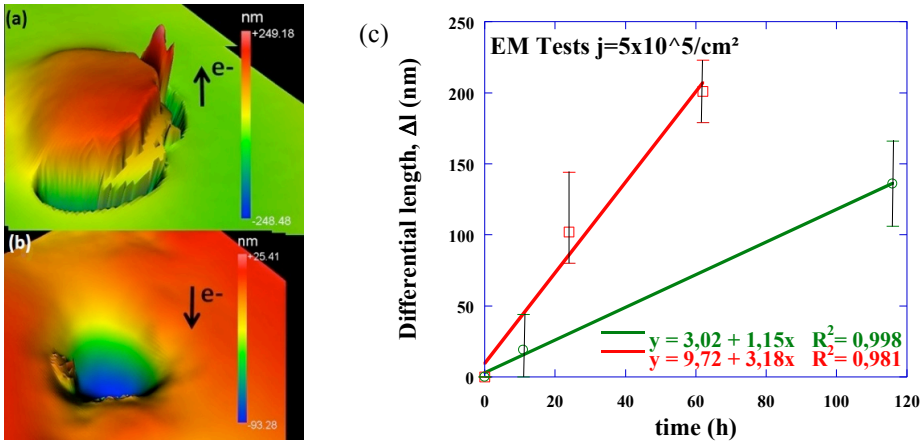

Figure 7: SWLI surface profiles of a TSV following EM exposure at 170°C for 24 hours: top (a) and bottm (b). Electron flow directions are indicated. (c) The top of the TSV protrudes progressively with time, and at a higher rate at higher temperature (red=170°C, green=120°C).

Figures 7a and 7b show SWLI profiles of the regions near the top and bottom surfaces of a TSV after EM testing at 170°C for 60 hours. It is clear that while the TSV protrudes from the surface of Si at the top, it intrudes into the Si at the bottom. Note that the current flows through this TSV from the top towards the bottom. Since the diffusive flux due to electromigration flows along the electron flow-direction, the flux flows from bottom to top. As a result, the entire TSV has migrated towards the top. While the EM flux can flow through the grain boundaries inside the Cu, because of the presence of relatively few grains through the diameter of the TSV, there is limited grain boundary area to promote EM. In contrast, the interface, being a very effective short circuit path for diffusion, is highly effective in accommodating the differential deformation or sliding between Cu and Si. **Figure 7c** shows the accrual of differential displacement between Cu and Si with increasing EM exposure time at two different temperatures (120°C and 170°C). As expected, there is more differential deformation at the higher temperature. It is also seen that interfacial sliding displacement continuously and linearly accrues with increasing EM time and current density

(j), which is proportional to the applied electric field E. An inspection of equation 1 shows that in the absence of a shear stress τ_i (or when τ_i is neglible), interfacial sliding can be driven only by the electric field, with the rate increasing with rising E (i.e., rising j) and rising temperature (because of the temperature-dependence of diffusivity). Thus, the observed effects are entirely consistent with the constitutive relation for diffusionally accommodated interfacial sliding.

In summary, it is evident that interfacial incompatibility may be of signficant concern in TSV structures, and therefore in 3D electronic devices. While this is important during thermal cycling, it is particularly important under EM conditions, since this damage keeps accummulating without attentuation with incresing time.

5 CONCLUSIONS

Thermal cycling (TC) and electromigration (EM) experiments were conducted on a chip containing 10μm TSVs under various conditions. It was observed that TC results in symmetric protrusion/extrusion of TSVs from both surfaces of the chip, whereas EM results in protrusion from one surface and intrusion into the other surface. The effects due to TC were simulated via finite element modeling (FEM), accounting for diffusionally accommodated interfacial sliding, as well as creep of Cu. It was found that the sharp and progressively accummulating interfacial incompatibility between Cu and Si can be explained by a creeping interfacial zone simulating a diffusionally sliding interface. While the interfacial incompatibility stabilizes during thermal cycling after a few cycles, it keeps accruing during EM. Thus the latter mechanism is a signficant potential source of reliability problems in 3D electronic devices.

10 ACKNOWLEDGMENTS

This research was supported by the National Science Foundation (DMR-1309843), Cisco Research Council (CRC), and the Missile Defense Agency. The authors are grateful to Cisco Systems for supplying the test samples.

REFERENCES

[1] S. Yoda, N. Kurihara, K. Wakashima and S. Umekawa, "Thermal Cycling Induced Deformation of Fibrous Composites with Particular Reference to the Tungsten-Copper System", *Metall. Trans.*, **9A**, 1978, pp. 1229-1236.

[2] I. Dutta, S. Mitra, A. D. Wiest, "Some Effects of Thermal Residual Stresses on the Strain Response of Graphite-Aluminum Composites during Thermal Cycling", in *Residual Stresses in Composites*, E.V. Barrera and I. Dutta, eds., TMS-AIME, Warrendale, Pennsylvania, 1993, pp. 273-292.

[3] J. V. Funn and I. Dutta, "Creep Behavior of Interfaces in Fiber Reinforced Metal-Matrix Composites", *Acta Mater.*, **47**, 1999, pp. 149-164.

[4] R. Nagarajan, I. Dutta, J.V. Funn and M. Esmele, "Role of Interfacial Sliding on the Longitudinal Creep Response of Continuous Fiber Reinforced Metal-Matrix Composites", *Mater. Sci. Engng.*, **A259**, 1999, pp. 237-252.

[5] I. Dutta, "Role of Interfacial and Matrix Creep During Thermal Cycling of Continuous Fiber Reinforced Metal-Matrix Composites", *Acta Mater.*, **48**, 2000, pp. 1055-1074.

[6] D. V. Zhmurkin, T.S. Gross and L.P. Buchwalter, "Interfacial Sliding in Cu/Ta/Polyimide High Density Interconnects as a Result of Thermal Cycling", *J. Electronic. Mater.*, **26**, 1997, p. 791.

[8] V. C. Jobin, R. Raj and S. L. Phoenix, "Rate Effects in Metal-Ceramic Interface Sliding from the Periodic Film Cracking Technique", *Acta Metall. Mater.*, **40**, 1992, pp. 2269-2280.

[9] S. Ankem & H. Margolin, "Alpha-Beta Interface Sliding in Ti-Mn Alloys", *Met. Trans. A*, **14A**, 1983, p. 500.

[10] S. Ankem & H. Margolin, "A Rationalization of Stress-Strain Behavior of Two Ductile Phase Alloys", *Met. Trans. A*, 1986, p. 2209.

[11] J. Rosler and A. G. Evans, "Effect of Reinforcement Size on the Creep Strength of Intermetallic Matrix Composites", *Mater. Sci. Engng.*, **A153**, 1992, pp. 438-443.

[12] R. S. Mishra, T. R. Bieler and A. K. Mukherjee, "Superplasticity in Powder Metallurgy Aluminum Alloys and Composites", Acta Metall. Mater., **43**, 1995, pp. 877-891.

[13] R. S. Mishra, T. R. Bieler and A. K. Mukherjee, "Mechanism of High Strain Rate Superplasticity in Aluminum Alloy Composites", *Acta Mater.*, **45**, 1997, pp.561-568.

[14] M. Ignat and R. Bonnet, "Role of the Phase Boundaries in the Hot Deformation in Tension of Al-$CuAl_2$ Single Eutectic Grains – A Deformation Model", *Acta Metall.*, **31**, 1983, pp. 1991-2001.

[15] D. Gupta, K. Vieregge and W. Gust, "Interface Diffusion in Eutectic Pb-Sn Solder", *Acta Mater.*, **47**, 1999, pp.5-12.

[16] L. M. Hsiung and T. G. Nieh, "Creep Deformation of Lamellar TiAl Alloys Controlled by Viscous Glide of Interfacial Dislocations", in 'Interstitial and Substitutional Solute Effects in Intermetallics', I. Baker, R. D. Noebe and E. P. George, eds., TMS, 1998, pp. 201-210.

[17] K. A. Peterson, I. Dutta and M.W. Chen, "Measurement of Creep Kinetics at Al-Si Interfaces", *Scripta Mater.*, **47** (2002) p. 649.

[18] K. A. Peterson, I. Dutta and C. Park, "Interfacial Creep in Multi-Component Material Systems", *J. Metals, Minerals and Materials Soc.* (JOM), **55**, no. 1 (2003) pp. 37-43.

[19] K. A. Peterson, I. Dutta and M.W. Chen, "Diffusionally Accommodated Interfacial Sliding in Metal-Silicon Systems", *Acta Mater.*, **51** (2003), pp. 2831-2846.

[20] K. A. Peterson, I. Dutta and M.W. Chen, "Processing and Characterization of Diffusion Bonded Aluminum-Silicon Interfaces", *J. Mater. Proc. Tech.*, **145** (2004), 99-108.

[21] M.W. Chen and I. Dutta, "Atomic Force Microscopy Study of Plastic Deformation and Interfacial Sliding in Al Thin Film : Si Substrate Systems due to Thermal Cycling", *Appl. Phys. Lett.*, **77** (2000) p.4298.

[22] I. Dutta, M.W. Chen, K. Peterson and T. Shultz, "Plastic Deformation and Interfacial Sliding in Al and Cu Thin Film: Si Substrate Systems Due to Thermal Cycling", *J. Electronic Mater.*, **30**, 2001, p.1537.

[23] I. Dutta, K. Peterson and M.W. Chen, "Plasticity and Interfacial Sliding in Cu Thin Film: Si Substrate Systems During Thermal Cycling", in Plasticity, Damage and Fracture at Macro, Micro and Nano Scales, Proc. *9th Int'l. Symp. on Plasticity*, A.S. Khan and O. Lopez-Pamies, eds., NEAT Press, MD, 2002, p.117.

[24] C. Park, I. Dutta and J. Vella "Interfacial Sliding and Deformation in Back-End Interconnect Structures in Microelectronic Devices", *J. Electronic Mater.*, **32** (2003), pp.

1059-1071.

[25] I. Dutta, K. A. Peterson and M.W. Chen, "Interfacial Sliding in Multi-Component Materials Systems and Its Mechanism", *Modelling the Performance of Engineering Structural Materials III*, T. S. Srivastan, D.R. Leseur and E.M. Taleff, eds., 2002, Proc. TMS Symp., pp. 253-267.

[26] C. Park, I. Dutta, K A Peterson, J. Vella, "AFM studies of Deformation and Interfacial Sliding in Interconnect Structures in Microelectronic Devices", *Materials, Technology and Reliability for Advanced Interconnects and Low-K Dielectrics*, Proc. MRS Spring Mtg., vol. **766**, 2003, pp. 385-390.

[27] I. Dutta, C. Park, K. A. Peterson, J. Vella and D. Pan, "Modeling of Interfacial Sliding and Film Crawling in Back-end Structures of Microelectronic Devices", *Proc. 9th Intersoc. Conf. on Thermal and Thermomechanical Phenomena in Electronic Systems*, IEEE/ASME, 2004, pp.137-144.

[28] C. Park, T. E. Shultz and I. Dutta, "An Environmentally Protected Hot-Stage AFM for Studying Thermo-mechanical Deformation in Microelectronic Devices", *Rev. Sci. Instrum.*, **75**, 2004, pp. 4662-4670.

[29] I. Dutta, C. Park, J. Vella and D. Pan, "Effect of Internal Stresses on Thermo-Mechanical Reliability of Interconnect Structures in Microelectronic Devices", *Mater. Sci. Eng. A*, **421**, 2006, pp 118-132.

[30] I. Dutta, P. Kumar and M. S. Bakir, "Interface-Related Reliability Challenges in 3-D Interconnect Systems with Through-Silicon Vias" *J. Metals*, **63**(10) (2011) 70-38.

[31] P. Kumar, I. Dutta and M. S. Bakir, "Interfacial Effects During Thermal Cycling of Cu-Filled Through-Silicon Vias (TSV)", *J. Elec. Mater.*, **41** (2012) 322 – 335.

[32] P. Kumar and I. Dutta, "Influence of electric current on diffusionally accommodated sliding at hetero-interfaces", *Acta Mater.*, **59** (2011) 2096-2108.

[33] J. M. E. Harper, C. Cabral Jr., P. C. Andricacos, L. Gignac, I. C. Noyan, K. P. Rodbell and C. K. Hu, "Mechanisms for microstructure evolution in electroplated copper thin films near room temperature", J. Appl. Phys., **86** (1999) p. 2516.